




Effect of the Al–CNT interlayer on the tensile elastic modulus of Al matrix composites with random dispersion of CNTs

L. Pérez¹ · I. Cabrera¹ · A. A. Santiago² · J. Vargas³ · A. Beltrán³ · I. Alfonso³ 

Received: 4 December 2017 / Accepted: 26 October 2018 / Published online: 1 November 2018
© The Brazilian Society of Mechanical Sciences and Engineering 2018

Abstract

This work studies the effect of Al_4C_3 layer formation in the carbon nanotube (CNT)–Al interface on the tensile elastic modulus of the resulting composite material, focusing on the thickness of this layer. 3-D models combining discrete element model and finite element analysis (FEA) were used in order to simulate the behavior of composites with different volume fractions of CNTs randomly dispersed into the Al matrix. Layers of 1, 5, 10 and 15 nm were modeled, affecting the CNTs according to the expected interfacial reaction. Estimations were compared to those obtained in a previous work using unit cell models for an ordered composite. Results showed that the presence of this interface increases total reinforcement volume fraction. Besides, elastic modulus of the composites increased with CNT volume fraction, while the increase in the interface thickness also provoked an increment in the Young's modulus, attributed to the combined reinforcement effect of CNT and Al_4C_3 . Estimations for the 3-D models were between maxima and minima values predicted by longitudinal and transversal moduli for ordered composites. Results also showed the importance of the use of more realistic FEA models for improving the predicting ability of this method for predicting the mechanical behavior of composites.

Keywords CNT · Al_4C_3 · Aluminum · FEA · DEM

1 Introduction

In the last decades, carbon nanotubes (CNTs) have been extensively used for reinforcing materials, which present properties that allow the use of such materials in different applications. Among the most important properties that are

improved with the insertion of the CNTs are the decrease in the density and the increase in mechanical and thermal properties [1–3]. The reinforcement of composites using CNTs has been mainly focused on polymer matrices (PMC), fact that has motivated important works [2, 4]. There is a wide variety of CNTs, including multiwalled tubes with Young modulus and strength up to 1000 GPa and 100 GPa, respectively [5]. This has led to the use of CNTs also as reinforcement in metal matrix composites (MMCs), mainly for aluminum matrices, obtaining materials characterized by higher specific strength, specific modulus, better fatigue resistance, better high-temperature response and better wear resistance [6]. These properties motivate the use of Al matrix composites for applications which need lower density without losing strength. Comparing to PMCs, there has been comparatively little research for the case of CNT–Al MMCs [7–10], needing a special attention the interfacial bonding between CNT and metallic matrix, mainly when molten metal is used in the manufacturing process. Powder metallurgy process has been also studied, but in this case interface formation is reduced due to the lower manufacturing temperature. The carbides formed and their characteristics have important effects on the mechanical behavior of these

Technical Editor: Paulo de Tarso Rocha de Mendonça, Ph.D.

✉ I. Alfonso
ialfonso@unam.mx

¹ Department of Mechanical Engineering, Universidad Técnica Federico Santa María, Av. España 1680, 110 Casilla, Valparaíso, Chile

² Escuela Nacional de Estudios Superiores, Unidad Morelia, Universidad Nacional Autónoma de México, Campus Morelia UNAM, Antigua Carretera a Pátzcuaro No. 8701, Col. Ex-Hacienda de San José de la Huerta, CP 58190 Morelia, Michoacán, Mexico

³ Instituto de Investigaciones en Materiales, Unidad Morelia, Universidad Nacional Autónoma de México, Campus Morelia UNAM, Antigua Carretera a Pátzcuaro No. 8701, Col. Ex-Hacienda de San José de la Huerta, CP 58190 Morelia, Michoacán, Mexico

materials. Different techniques have been used in order to study these interfaces, mainly including microscopy (scanning electron microscopy, SEM; and transmission electron microscopy, TEM [7, 10]). The literature shows that matrix composition has a significant effect on the interfacial layer formed due to the reaction between CNT and molten metal, e.g., Al_4C_3 or SiC for Al alloys with different Si contents [11]. According to this, the thickness and composition of the interface significantly affect the mechanical properties of the composites, as the strength and thickness of the carbides determine the stress that could be transferred to the CNT. There are reported different thicknesses for the carbide layer differs: Bakshi et al. [11] found that for an Al–11%Si alloy it is approximately 6 nm, while He et al. [7] showed that starting from CNTs of 5–20 nm in diameter in contact with Al it is possible to obtain Al_4C_3 nanowires ranging from 7 to 25 nm. Al_4C_3 presents both perpendicular and lateral growth separated into two steps: initially, the formation of a thin carbide coating; followed by the consumption of the CNT until the formation of an Al_4C_3 layer [7]. Then, the study of this phenomenon is essential for a better study of the resulting composites. There are numerous analytical and numerical models for the prediction of mechanical behavior of composite materials and interfaces [3, 12], which involve different important assumptions and the selection of a uniform representative volume element (RVE) which captures a minimum repeatable feature that represents the microstructure. The mechanical properties of the composites also depend on different characteristics of the reinforcement, such as volume fraction, aspect ratio, size and distribution, orientation and interfaces [1]. Then, the growing mechanism and the possible interface thickness are essential data for the selection of the model that needs to include the combination reinforcement–interface–matrix. Among these models is rule of mixtures, which evaluates the effective elastic response of a composite under axial load. Even different reinforcements or phases can be included, as is the case of an interlayer. Nevertheless, it does not consider the random distribution of the reinforcements, their aspect ratio and other aspects related to the configuration of the composite. Due to its modeling capability, finite element analysis (FEA) is one of the most important methods used to analyze the mechanical behavior of composites, being able to include characteristics such as the array and aspect ratio of the reinforcements, and the presence of interlayers (as in the case of Al_4C_3 for CNT-reinforced aluminum matrix composites) [10–14]. Following this trend, the interface thickness and volume fraction effect on the elastic modulus of CNT-reinforced PMCs have been studied for several researches [14, 15]. Nevertheless, few works study the carbide interfaces for MMCs, just analyzing the effect of the interface stiffness, thickness and debonding for general cases [7, 8, 16, 17]. These works do not analyze the effect of the Al_4C_3 interlayer on the elastic modulus,

neither including the analysis of the formation of the interfaces, as could be the CNT and matrix consumption due to the interface growing, and the final characteristics of the resulting reinforcement (CNT + layer).

Based on the latter, a previous work [18] studied the effect of the CNT– Al_4C_3 -matrix system on the elastic modulus of MMCs with different volume fractions, modeling a unitary cell with only one CNT as RVE. Nevertheless, this work was an introductory study case, just analyzing the case of ordered MMCs, being necessary to extend the analysis to randomly distribute CNTs and RVEs including more than one unit cell. Combining DEM and FEA, it is possible to reach this goal. With the use of the DEM, randomly distributed CNTs can be generated in a first step in order to better reproduce their distribution [18]. This allows to obtain just the center of each CNT as x , y , z coordinates (modeled first as spheres), controlling the distance between these centers for modeling in a second stage the CNT. The use of DEM provides several advantages: One of them could be reduction in computer requirements. Once the model for CNTs distribution is ready, a second important aspect is the number of CNTs that needs to be included in each FEA model. Computations convergence for these models has been analyzed in other works finding that RVEs must be at least ~ 2.5 – 3.5 times the maximum size of certain feature that represents the material (unit cell) [19]. Then, in order to improve the results obtained in the mentioned previous work, the selected size of the RVE in a new work should be at least equivalent to the length of 2.5–3.5 CNTs. This DEM–FEA model will be closer to the real composites morphologies, providing estimations in better agreement with experimental results. That is why the present work is focused to analyze, using DEM–FEA, the effect of the Al_4C_3 interface thickness on Young's modulus (E) for aluminum matrix composites reinforced with different volume fractions of randomly dispersed CNTs.

2 Models and calculation

2.1 Generation of random distributions for CNTs

Open-source DEM simulation software LIGGGHTS[®] [20] was used in order to generate randomly distributed coordinates for CNTs location, being the initial stage of the modeling process. This first step consists of ascertaining the behavior of spherical particles immersed into a 4- μm -diameter (d) and 3.2- μm -height (h) cylinder with the aspect ratio $h/d = 0.8$. The used criterion for selecting this size was needed for computations convergence already mentioned (at least the length of 2.5–3.5 CNTs). Depending on the CNT volume fraction, a certain number of spheres were inserted. The conditions for the interactions between these inserted particles were selected just to generate a high

interaction between them and to get the desired random distribution. In order to obtain repetitive results, three DEM random distributions were obtained for each model for CNTs, reporting as Young's modulus the average obtained using these distributions. In Fig. 1a, b, two examples of random distributions of the spheres used for the models can be observed.

2.2 Finite elements models for the MMCs (CNT– Al_4C_3 matrix system)

Once the coordinates were obtained by DEM, they were post-processed in order to generate scripts using commercial FEA software ANSYS 16.0, followed by the creation of CAD models. CNTs were located at the generated coordinates, modeled as solid cylinders with open ends, with 0.070 μm in diameter and 1 μm in height, and the aspect ratio 14 ($L/D = 1000/70$ nm) [10]. The selected volume fractions for the inserted CNTs ranged from 0.02 to 0.2. These small quantities were selected in order to optimize the computational requirements. The matrix used for modeling purposes corresponds to Al–12 wt% Si, as the one obtained by Lasagni et al. [17] using a squeeze casting process, with a typical Young's modulus of 77 GPa, and a Poisson coefficient of 0.33, already used in a previous work [18]. Young's modulus and Poisson's ratio of the CNTs were 680 GPa and 0.27, respectively, which correspond to multiwalled CNTs with outer and inner radii of 35 and 15 nm, respectively [21]. In order to obtain more realistic models, the effect of the Al_4C_3 –CNT interface was included according to the

analysis developed in a previous work [18], where Al_4C_3 layers with thicknesses of 1, 5, 10 and 15 nm were included for CNTs with and without end caps, using separately in the axisymmetric model the areas and mechanical properties of the CNTs and the Al_4C_3 layers. In the mentioned work, the CNT volume consumed during the interfacial reaction with the Al alloy was estimated, resulting in a total diameter for the resulting reinforcements (CNT + Al_4C_3). According to Bakshi et al. [5], the reaction occurs on all the CNT surface, perpendicularly growing the carbide governed by the diffusion of Al and C through Al_4C_3 . This condition of chemical bonding is treated in FEA as perfect adhesion between CNT, Al_4C_3 and matrix, fact that was assumed in the present work linking FEA elements of the different materials through the “add” command of ANSYS 16.0. The presence of the interlayer affected the relative volume fractions in the composite for the matrix and the reinforcement. In the present work, we are modeling the system CNT + Al_4C_3 as single cylinders of different diameters depending on the interface thickness, each one with unique mechanical properties calculated according to the relative quantities of the CNT and the Al_4C_3 interface in the cylinder (as for the CNT, with 1 μm in length). Cylinder radii, Young's moduli and Poisson coefficients for the reinforcements (CNT + Al_4C_3) are shown in Table 1 for different layer thicknesses. For determinations, the properties used for Al_4C_3 were: Young's modulus of 309 GPa and a Poisson coefficient of 0.20 [22]. As can be observed, the reinforcement (CNT + Al_4C_3) radius is not obtained just by adding the layer thickness to the outer radius of a CNT (35 nm), but taking into account the fact

Fig. 1 Spheres distributions used to generate coordinates for CNTs for volume fractions of **a** 0.05 and **b** 0.1

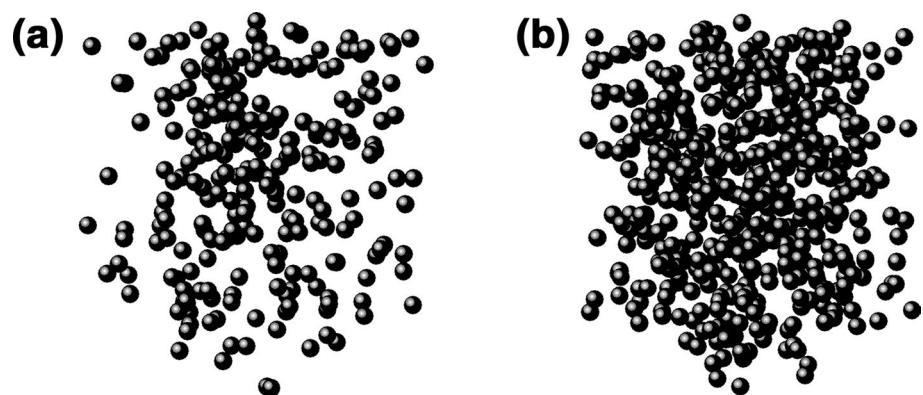


Table 1 Reinforcement radius, aspect ratio and mechanical properties for CNTs with different Al_4C_3 layers

Al_4C_3 layer thickness (nm)	Reinforcement radius, CNT + Al_4C_3 (nm)	Reinforcement aspect ratio	Young's modulus (GPa)	Poisson coefficient
1	35.26	14.18	655	0.265
5	38.25	13.07	573	0.250
10	41.35	12.09	497	0.235
15	44.28	11.29	443	0.225

that interface grows consuming not only Al matrix but also the CNT, fact that decreases the volume fractions for the CNT and the matrix. Nevertheless, the sum CNT–interface volume fraction always increases.

Figure 2a, b shows examples of modeled cylindrical specimens with two different CNT volume fractions, engendered through DEM–FEA combination. As can be observed, the distributions of the CNTs are random. Their directions were obtained through the generation of three random angles for obtaining x , y and z directions.

2.3 Simulation for the MMCs

The Young's moduli of the MMCs with different reinforcement volume fractions were uniaxially estimated when applying equivalent compressive displacements on the

nodes of the upper end of the cylindrical specimens. Ten-node tetrahedral structural solid elements were employed for meshing. The number of nodes ranged from 2×10^5 to 2×10^7 , while the number of elements from 2×10^4 to 6×10^6 , increasing these quantities with the increase in the CNT volume fraction. Mesh convergence analysis was carried out by gradually increasing the number of elements and verifying the local stress behavior to ensure convergence of the numerical solution. The coupled-node boundary condition (keeping the nodes in the same plane) was used for the upper face of the cylinder. The reinforcements were meshed in complete contact with the matrix. Figure 3a, b shows the meshed model for the reinforcements (CNT + Al_4C_3) resulting in interfaces of different thicknesses.

Fig. 2 FEA models of MMCs reinforced with volume fractions of 0.02 (CNTs + Al_4C_3) and interfaces of **a** 1 nm and **b** 15 nm

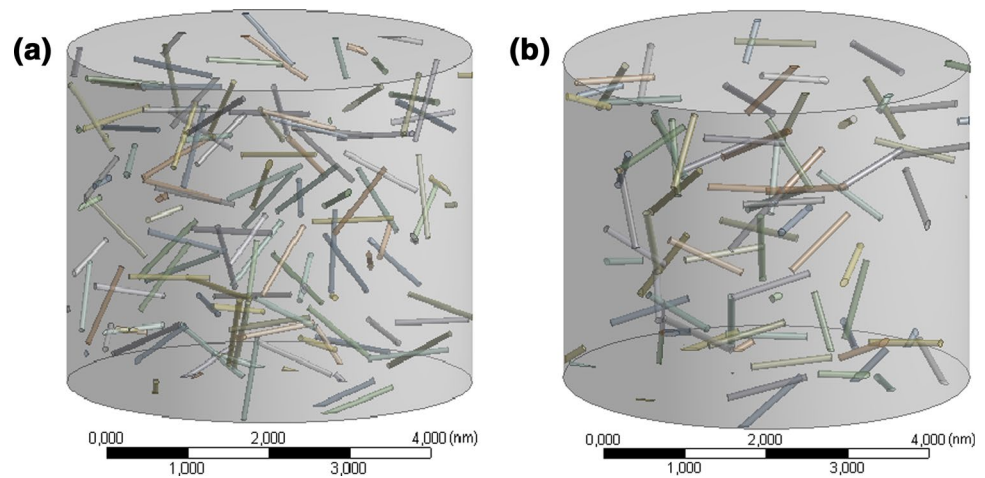
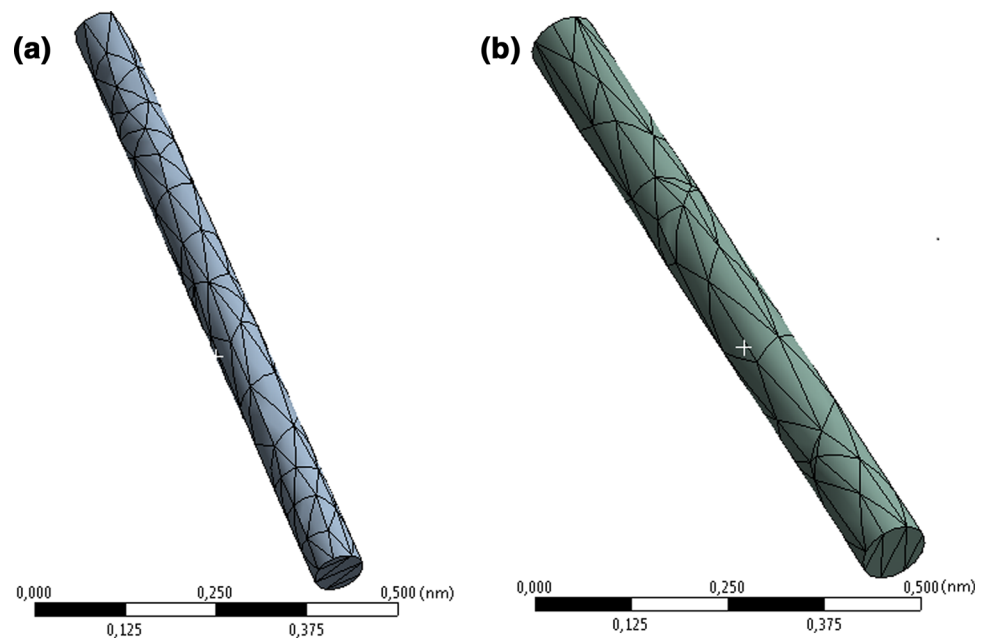


Fig. 3 Meshing for isolated reinforcements (CNT + Al_4C_3) with interfaces of **a** 1 nm (total radius 35.26 nm), and **b** 15 nm (total radius 44.28 nm)



Young’s modulus can be obtained from the response of the simulated compression test, and along the z -axis (E_z), it can be determined by:

$$E_z = \frac{\sigma_z}{\epsilon_z} \tag{1}$$

where σ_z and ϵ_z are the stress and the strain in z -axis, respectively. The displacement applied (1% of h) to the cylinder in z -axis (u_z is used for the strain determination) is:

$$\epsilon_z = \frac{u_z}{L_z} \tag{2}$$

where L_z is the original height of the cylindrical specimen. The stress necessary for solving Eq. 1 is determined using the following equation:

$$\sigma_z = \frac{F_z}{A} \tag{3}$$

where F_z is the reaction force in the z -axis obtained through the FEA simulation, for the nodes of the bottom end of the cylindrical specimens; while A is the area of this surface.

3 Results and discussion

Figure 4a shows the meshed structure for a modeled composite with 0.05 volume fraction of CNTs with nanolayers of 5 nm, where reinforcements can be easily observed (circled), while Fig. 4b shows, for the same composite, the graphical response for the total deformation originated due to the applied displacements. In this figure, the uniform response of the x - y surfaces can be noted.

The effects of the reinforcement volume fraction and the interface thickness on the Young’s modulus can be observed in Fig. 5a. The increase in the CNT volume fraction provoked important rises in the Young’s modulus from values of approximately 85 GPa for a CNT volume fraction of 0.02 to more than 110 GPa for a volume fraction of 0.20. This behavior is observed for both CNTs and CNT + Al_4C_3 due to the fact that in both cases reinforcements have higher Young’s modulus than the Al matrix. In Fig. 5b, it can be observed that the increase in the Al_4C_3 nanolayer leads to higher values of the Young’s modulus, mainly for high thicknesses, reaching a maximum of 127 GPa for a MMC with a volume fraction of 0.2 and a nanolayer of 15 nm (12% higher than for the CNT without Al_4C_3). This behavior agrees well

Fig. 4 **a** Meshed model for composite with 0.05 volume fraction of CNTs with nanolayers of 5 nm and **b** total deformation distribution originated due to the applied displacement

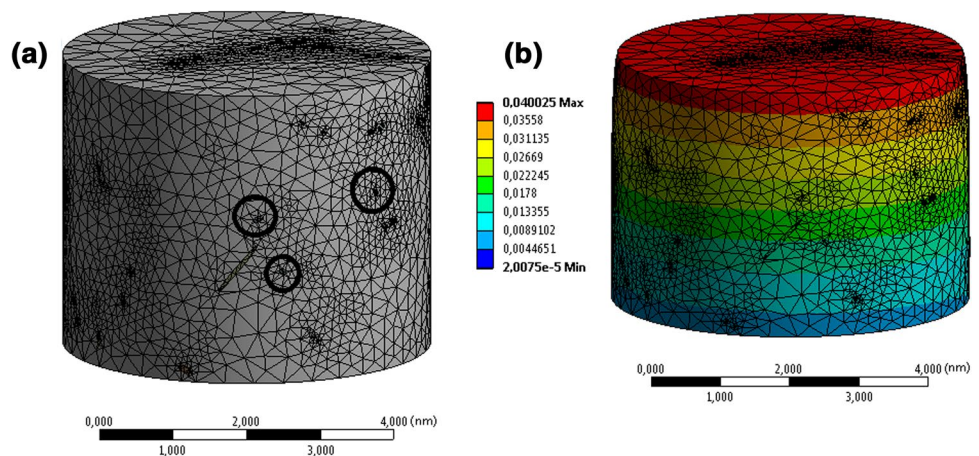
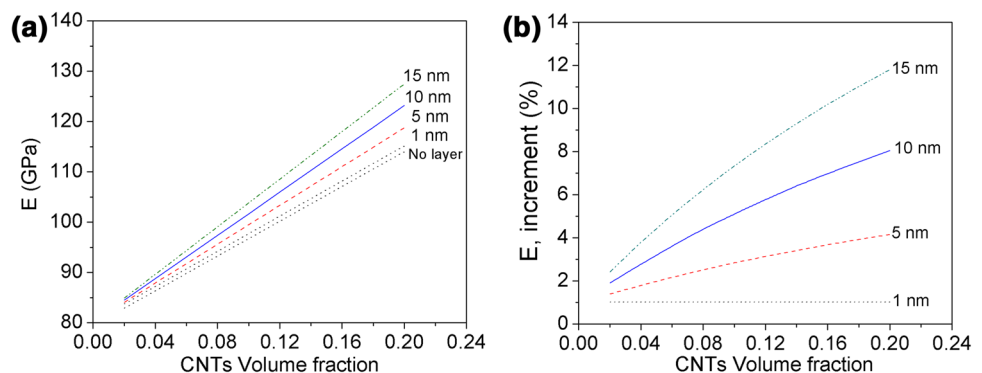


Fig. 5 **a** Multicell FEA-estimated Young’s modulus (E) versus CNT volume fraction and **b** increment percentage for E , depending on the thickness of the interfacial Al_4C_3 layer



with the one obtained in a previous work, where unit cell RVE was used [18], and with other experimental results, which reported that the formation of nanosize layers of Al_4C_3 at the interface is beneficial for the mechanical properties of composites by increasing the interfacial bonding [23], helping in load transfer to CNT by pinning the nanotubes to the matrix [24]. Besides, the formation of the Al_4C_3 nanolayer contributes to an increase in the total quantity of reinforcement, which increases for higher Al_4C_3 thicknesses.

Figure 6a depicts the Young's modulus behavior for FEA models using: (1) a unit cell [18] for the case of CNTs without end caps and (2) randomly distributed 3-D multicells obtained in this work, both with different interface thicknesses. As can be observed, results for multicell models are located in the range between maximum (longitudinal) and minimum (transversal) Young's moduli obtained for the unit cell model. Experimental characterizations are generally located in this range, so, the results estimated using the multicell models are in excellent agreement with the expected one. It is important to remark that the differences observed for the composites using different thicknesses are more significant for the case of models using multicells and for the transversal direction for models with unit cells. This increase is more important than that observed for the longitudinal case when a unit cell is used, fact that could be explained due to the dominant effect of the high aspect ratio of the reinforcements when this direction is used. Besides, it has been reported that CNTs may not be as effective as long CNTs in reinforcing a composite [15]. Otherwise, Fig. 6b shows the percentage differences between the estimations obtained using the 3-D models and the average values obtained using longitudinal and transversal Young's moduli for unit cell models. As can be observed, the above-mentioned effect of the high CNTs aspect ratio leads to overestimations of the Young's moduli when ordered models are used, reaching a maximum of 28%. The predominant effect of the aspect ratio in a certain direction is avoided using random multicell models. It can be also observed that the overestimation of E slightly decreases with the increase in the interlayer thickness (22% for CNTs with an Al_4C_3 layer

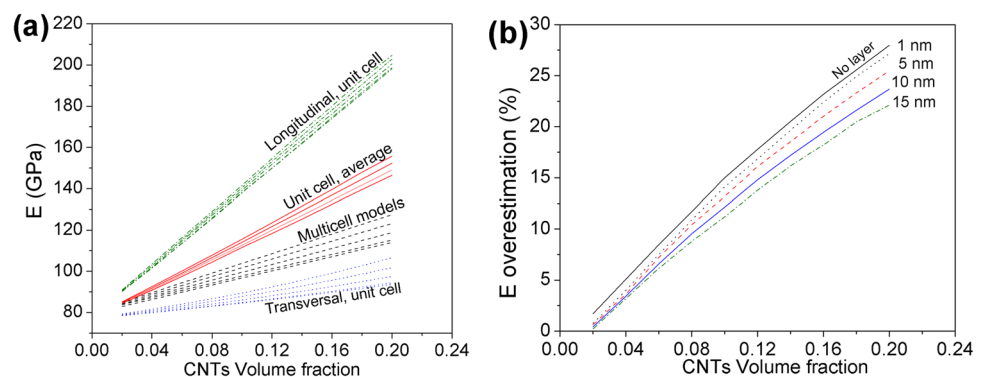
of 15 nm and volume fraction of 0.2). A plausible explanation to this behavior is the modification originated in the reinforcement aspect ratio, which decreases from 15.6 for the CNT without Al_4C_3 to 11.29 for CNTs with interlayers of 15 nm, as already observed in Table 1. These lower aspect ratios lead to a slight diminution in the predominant effect of the Young's moduli estimated in the longitudinal direction, increasing the contribution of the transversal analysis. If the case of CNTs with end caps was modeled and compared with [18], the expected behavior could be similar to the one obtained in the present work, being the Young's moduli in the same range for multicell estimations, because when short CNTs are used, the difference between cases with and without end caps is less than 5% [15]. It is also important to remark that these models could be used for the study of CNTs without interlayers, as the obtained processing MMC by powder metallurgy, where interfacial Al–CNT reaction is not favored. This condition in FEA would be studied without “adding” different materials, far different from the case when chemical bonding exists, where FEA elements of different materials are linked.

4 Conclusions

After the analysis of the compressive response of Al–Si/CNT MMCs with Al_4C_3 interfaces, comparatively studied using unit cell and randomly distributed multicell FEA models, the following can be concluded:

- The use of multicell random models generated using a DEM–FEA combination made it possible to realize more realistic models of CNT-reinforced composites.
- For both, CNT and CNT + Al_4C_3 composites, estimated elastic moduli significantly linearly increased as the CNT volume fraction increased.
- Young's modulus increased with the increase in the Al_4C_3 interlayer thickness, reaching a maximum increment of 15%, and being more significant for multicell models.

Fig. 6 **a** Young's moduli variation versus CNT volume fraction, for FEA estimations obtained using unit cell and randomly distributed multicell models, depending on the thickness of the interfacial Al_4C_3 layer and **b** Young's moduli overestimations when unit cell models are used compared to multicell models



- Young's modulus estimations using 3-D randomly distributed multicell FEA models were between maxima and minima values predicted by the longitudinal and transversal moduli for unit cell ordered models.
- The selection of the correct MMC topology has been demonstrated to be an essential variable for obtaining better estimations.

Acknowledgements L. Pérez acknowledges the financial support from the Advanced Center for Electrical and Electronic Engineering, AC3E, Basal Project FB0008, CONICYT. I. Alfonso would like to acknowledge the financial support from UNAM PAPIIT IN117316.

References

1. Everett RK, Arsenault RJ (eds) (1991) Metal matrix composites: processing and interface. Academic Press, New York
2. Park SH, Bandaru PR (2010) Improved mechanical properties of carbon nanotube/polymer composites through the use of carboxyl-epoxide functional group linkages. *Polymer* 51(22):5071–5077. <https://doi.org/10.1016/j.polymer.2010.08.063>
3. Hashin Z, Rosen BW (1965) The elastic moduli of fiber-reinforced materials. *J Appl Mech* 31(2):223–232. <https://doi.org/10.1115/1.3629590>
4. Yu N, Chang YW (2008) Effects of CNT diameter on the uniaxial stress-strain behavior of CNT/epoxy composites. *J Nanomater* 2008:1–6. <https://doi.org/10.1155/2008/834248>
5. Bakshi SR, Lahiri D, Agarwal A (2010) Carbon nanotube reinforced metal matrix composites: a review. *Int Mater Rev* 55(1):41–64. <https://doi.org/10.1179/095066009X12572530170543>
6. Umma A, Maleque MA, Iskandar IY, Mohammed YA (2012) Carbon nano tube reinforced aluminium matrix nano-composite: a critical review. *Aust J Basic Appl Sci* 6(12):69–75
7. He CN, Zhao NQ, Shi CS, Song SZ (2010) Fabrication of aluminum carbide nanowires by a nano-template reaction. *Carbon* 48(4):931–938. <https://doi.org/10.1016/j.carbon.2009.10.004>
8. Laha T, Kuchibhatla S, Seal S, Li W, Agarwal A (2007) Interfacial phenomena in thermally sprayed multiwalled carbon nanotube reinforced aluminum nanocomposite. *Acta Mater* 55(3):1059–1066. <https://doi.org/10.1016/j.actamat.2006.09.025>
9. Noguchi T, Magario A, Fukazawa S, Shimizu S, Beppu J, Seki M (2004) Carbon nanotube/aluminium composites with uniform dispersion. *Mater Trans* 45(2):602–604. <https://doi.org/10.2320/matertrans.45.602>
10. Simões S, Viana F, Reis Marcos AL, Vieira MF (2014) Improved dispersion of carbon nanotubes in aluminum nanocomposites. *Compos Struct* 108:992–1000. <https://doi.org/10.1016/j.compsstruct.2013.10.043>
11. Bakshi SR, Keshri AK, Singh V, Seal S, Agarwal A (2009) Interface in carbon nanotube reinforced aluminum silicon composites: thermodynamic analysis and experimental verification. *J Alloy Compd* 481(1–2):207–213. <https://doi.org/10.1016/j.jallcom.2009.03.055>
12. Frantziskonis GN (1994) Fiber-matrix interface: information from experiments via simulation. *Compos Struct* 29(3):231–247. [https://doi.org/10.1016/0263-8223\(94\)90021-3](https://doi.org/10.1016/0263-8223(94)90021-3)
13. Cook RD, Malkus DS, Plesha ME (1989) Concepts and applications of finite element analysis, 3rd edn. Wiley, New York
14. Al Masud M, Masud AKM (2010) Effect of interface characteristic and property on axial modulus of carbon nanotube based composites. *J Mech Eng* 41(1):15–24. <https://doi.org/10.3329/jme.v41i1.5358>
15. Joshi UA, Joshi P, Harsha SP, Sharma SC (2010) Evaluation of the mechanical properties of carbon nanotube based composites by finite element analysis. *Int J Eng Sci Technol* 2(5):1098–1107
16. Ahmadi I, Aghdam MM (2010) Analysis of micro-stresses in the SiC/Ti metal matrix composite using a truly local meshless method. *Proc Inst Mech Eng Part C J Mech Eng Sci* 224(8):1567–7. <https://doi.org/10.1243/09544062jmes1888>
17. Lasagni F, Degischer HP (2010) Enhanced Young's modulus of Al-Si alloys and reinforced matrices by co-continuous structures. *J Compos Mater* 44(6):739–755. <https://doi.org/10.1177/0021998309347649>
18. Alfonso I, Navarro O, Vargas J, Beltrán A, Aguilar C, González G, Figueroa IA (2015) FEA evaluation of the Al₄C₃ formation effect on the Young's modulus of carbon nanotube reinforced aluminum matrix composites. *Compos Struct* 127:420–425. <https://doi.org/10.1016/j.compstruct.2015.03.032>
19. Sebsadji SK, Chouicha K (2012) Determining periodic representative volumes of concrete mixtures based on the fractal analysis. *Int J Solids Struct* 49:2941–2950. <https://doi.org/10.1016/j.ijsolstr.2012.05.017>
20. Pérez L, Lascano S, Aguilar C, Estay D, Messner U, Figueroa IA, Alfonso I (2015) DEM-FEA estimation of pores arrangement effect on the compressive Young's modulus for Mg foams. *Comput Mater Sci* 110:281–286. <https://doi.org/10.1016/j.commat.2015.08.042>
21. Ding W, Calabri L, Kohlhaas KM, Chen X, Dikin DA, Ruoff RS (2007) Modulus, fracture strength, and brittle vs. plastic response of the outer shell of arc-grown multi-walled carbon nanotubes. *Exp Mech* 47(1):25–36. <https://doi.org/10.1007/s11340-006-9344-6>
22. Wen XX, Long H, Xiao Y, Zun-Ming L, Ying F, Yang-Xian L, Cheng-Chun T (2011) Ab initio study of the electronic structure and elastic properties of Al₅C₃N. *Chin Phys B* 20(12):126201:1–6. <https://doi.org/10.1088/1674-1056/20/12/126201>
23. Tham LM, Gupta M, Cheng L (2001) Effect of limited matrix-reinforcement interfacial reaction on enhancing the mechanical properties of aluminium-silicon carbide composites. *Acta Mater* 49(16):3243–3253. [https://doi.org/10.1016/S1359-6454\(01\)00221-X](https://doi.org/10.1016/S1359-6454(01)00221-X)
24. Kwon H, Estili M, Takagi K, Miyazaki T, Kawasaki A (2009) Combination of hot extrusion and spark plasma sintering for producing carbon nanotube reinforced aluminum matrix composites. *Carbon* 47(3):570–577. <https://doi.org/10.1016/j.carbon.2008.10.041>